THE JOURNAL OF PHYSICAL CHEMISTRY Letters

LETTER

pubs.acs.org/JPCL

Supramolecular Structures of Enzyme Clusters

Nadeem Javid,[†,‡] Karsten Vogtt,[§] Sangita Roy,[†] Andrew R. Hirst,[⊥] Armin Hoell,[#] Ian W. Hamley,[▽] Rein V. Ulijn,[†] and Jan Sefcik*[,‡]

[†]WestCHEM, Department of Pure & Applied Chemistry and [‡]Department of Chemical and Process Engineering, University of Strathclyde, Glasgow G1 1XJ, United Kingdom

[§]Institute for Soft Matter and Functional Materials, Helmholtz-Zentrum Berlin, 14109 Berlin, Germany

[⊥]School of Physics and Astronomy, University of Leeds, Leeds LS2 9JT, United Kingdom

[#]Institute of Applied Materials, Helmholtz-Zentrum Berlin, 12489 Berlin, Germany

[▽]Department of Chemistry, University of Reading, Whiteknights, Reading RG6 6AD, United Kingdon

ABSTRACT: The structural characterization of subtilisin mesoscale clusters, which were previously shown to induce supramolecular order in biocatalytic self-assembly of Fmoc−dipeptides, was carried out by synchrotron small-angle X-ray, dynamic, and static light scattering measurements. Subtilisin molecules self-assemble to form supramolecular structures in phosphate buffer solutions. Structural arrangement of subtilisin clusters at 55 °C was found to vary systematically with increasing enzyme concentration. Static light scattering measurements showed the cluster structure to be consistent with a fractal-like arrangement, with fractal dimension varying from 1.8 to 2.6 with increasing concentration for low to moderate enzyme concentrations. This was followed by a structural transition around the enzyme concentration of 0.5 mg mL^{-1} to more compact structures with significantly slower relaxation dynamics, as evidenced by dynamic light scattering measurements. These concentration-dependent supramolecular enzyme clusters provide tunable templates for biocatalytic self-assembly.

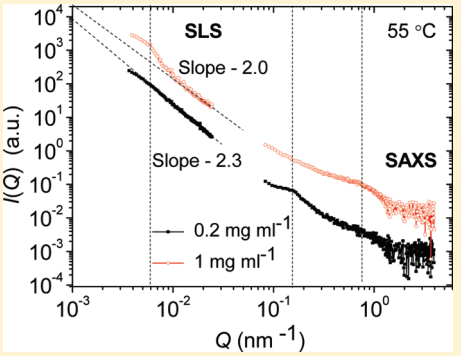

SECTION: Macromolecules, Soft Matter

Supramolecular self-assemblies with well-ordered structures and few defects are potential candidates for the next generation of advanced bionanomaterials due to their applications in diverse fields like healthcare and energy-related technologies.[1−6] The major challenge in the production of these materials is reliable and rapid self-assembly with minimal kinetic defects. The levels of organization achieved are dictated by a number of factors, including the balance among intermolecular interactions, the solution environment, geometric templating, and mass transfer.[7] A number of enzyme types, including esterases, proteases, and phosphatases, have been used to control the molecular self-assembly. These enzymes switch on a molecular cascade by structural modification of nonassembling precursors to self-assembling molecular entities that transform to self-assembled structures.[2]

In a recent study,[3] we made the counterintuitive observation that the level of order obtained in one of these systems (as evidenced by several spectroscopy and microscopy methods) shows a positive correlation with the concentration of catalyst used. This was unexpected as one would expect faster self-assembly rates to result in more, rather than fewer, defects, as has indeed been observed in salt-induced assembly of beta-hairpin-based hydrogels.[8] The key to this difference in behavior is likely linked to the unique nucleation and growth mechanisms observed in biocatalytic self-assembly involving poorly soluble peptide gelators, where the biocatalyst can act as a spatial confinement for the early nucleation stage of self-assembly by localizing the precursors and achieving a local concentration above the critical aggregation concentration.[9] It was proposed that enzyme molecules act cooperatively within clusters and that these clusters have lower mobility and higher rigidity due to more extensive networking at higher enzyme concentrations, as confirmed by dynamic light scattering measurements.[3] This clustering and lowered mobility may help to reduce discontinuities in fibrillar self-assembly and yield better ordered structures. Due to the important and unexpected role of catalytic clusters in these systems, these warranted further investigation. In the current Letter, we provide a structural characterization of the enzyme clusters formed using synchrotron small-angle X-ray, dynamic, and static light scattering measurements.

The use of enzymes for localized formation of nanostructures has also been described in the formation of inorganic structures. Matsui et al. demonstrated that crystalline ZnO nanoshells could be synthesized by using urease as a nanoreactor by exploiting the

Received: April 2, 2011
Accepted: May 18, 2011
Published: May 18, 2011

local pH change around the enzyme molecule.[10] Formation of protein clusters has been observed before. Various proteins have been shown to spatially order themselves into self-assembled clusters due to the balance of long-range repulsive and short-range attractive interactions. These interactions mainly arise from electrostatic and dispersion interactions due to protein structure or the presence of cosolvents and cosolutes in the bulk medium.[11,12] Enzymes have been shown to self-associate by changing pH, temperature, pressure, and concentrations, which can have either adverse or propitious effects on enzyme activity. Homogeneous solutions of lysozyme at pH = 4.5 with volume fractions as low as 0.016 were found to contain networks of weakly bound chains of protein molecules with relatively short characteristic lifetimes.[13] The multifunctional Calmodulin kinase II holoenzyme, which regulates diverse cellular processes, forms loosely packed clusters, and their further self-association upon changing pH from 7.5 to below 7.0 yields large networks of micrometer size. This self-association contributes to translocation and inactivation of the enzyme.[14] The enzyme subtilisin Carlsberg aggregates in organic solvents to clusters of about 60 molecules. Interestingly, it has been shown that these aggregates have enhanced activity and can provide a microenvironment for catalysis.[15] It has also been suggested that the mineralization of biosilica structures of glass sponge is templated on hydroxyl collagen (a naturally occurring protein), revealed by the presence of an unusual motif of hydroxylated fibrillar collagen obtained by slow alkali etching of biosilica.[16]

Despite the fact that the enzyme (protein) molecules themselves can act as geometric constraints/confinements, which directs complexity and higher order and fewer defects in self-assembled structures, we are not aware of any previous studies on the structural arrangements of enzyme clusters in the solution phase. In this study, we analyze the structure of supramolecular clusters of enzyme subtilisin using synchrotron small-angle X-ray scattering (SAXS), dynamic, and static light scattering. We show that enzyme molecules self-assemble into extensive fractal-like clusters with structural arrangements systematically depending on the enzyme concentration. These supramolecular structures then act as templates that may be used to direct biocatalytic self-assembly.

We have demonstrated in a recent study[3] that subtilisin self-associates in phosphate buffer solutions to extended clusters at 55 °C, which is the optimal temperature where it exhibits the highest biocatalytic activity. This was evidenced by dynamic light scattering measurements through the presence of decreased initial decay rates of density fluctuations and increased prominence of slow relaxation modes with increasing enzyme concentration. It was proposed that extended interconnected networks are formed in the enzyme solutions, which become more rigid with enhanced degree of interconnection at higher concentration. In order to further investigate subtilisin clustering in phosphate buffer solutions, we performed synchrotron SAXS measurements at different concentrations of subtilisin, which exhibited distinctly different relaxation times at 55 °C, as shown by dynamic light scattering.

First, we performed measurements at 25 °C in order to assess self-association of subtilisin in solutions at ambient conditions where the biocatalytic activity is not optimal. The background-corrected SAXS intensity measured at ambient temperature along with the calculated scattering intensity of monomeric subtilisin (form factor $P(Q)$ computed using the CRYSOL[17] software for the crystal structure of subtilisin based on its PDB entry 1BE8) is shown in Figure 1. The Guinier analysis for the theoretical form factor $P(Q)$ of the monomeric subtilisin yields the radius of gyration (R_g) of 1.8 nm.

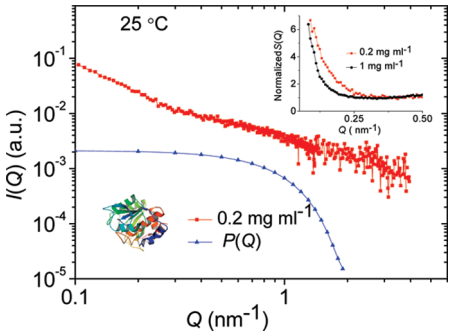

Figure 1. SAXS intensity (in au) measured for subtilisin (0.2 mg mL^{-1}) in phosphate buffer at 25 °C along with the calculated form factor $P(Q)$ for subtilisin monomer based on its crystal structure (PDB entry 1BE8). Normalized low Q structure factors $S(Q)$ for two different concentrations of subtilisin (0.2 and 1 mg mL^{-1}) are shown in the inset.

Normalized structure factors $S(Q)$ (inset in Figure 1) for subtilisin solutions at two different concentrations are significantly increasing at low Q values, which is consistent with the presence of clusters of much larger dimension than that of the monomeric subtilisin, even at ambient temperature. Dynamic light scattering measurements on subtilisin solutions at 25 °C showed a single nearly exponential decay of the autocorrelation function, indicating a relatively narrow distribution of decay rates independent of subtilisin concentration for a range of concentrations from 0.05 to 0.8 mg mL^{-1} (data not shown). Further measurements were done at 55 °C, which is the temperature where subtilisin shows the maximum biocatalytic activity and which is also the temperature that was used in our previous biocatalytic self-assembly work.[3] The dynamics of subtilisin clusters for various concentrations of subtilisin was again followed by dynamic light scattering, and the normalized autocorrelation functions are shown in Figure 2a. For comparison, we also show the theoretical autocorrelation function for monomeric subtilisin (R_h of about 2 nm) assumed to be subject to free diffusive motion.

The apparent diffusion coefficients calculated from the initial decay rate of the autocorrelation function using the cumulant method are shown in Figure 2b. The corresponding apparent mean hydrodynamic radius at low enzyme concentrations is very similar at both temperatures (with an R_h of about 80 nm) because the solvent viscosity at 55 °C is about twice lower than that at 25 °C. It can be seen that, unlike at ambient conditions, the cluster dynamics at 55 °C is concentration-dependent, with decreased initial decay rates of density fluctuations and slow relaxation modes becoming more apparent at higher concentration, as observed previously.[3] The appearance of slow decay modes at lag times of $\tau > 10^{-3}$ s in normalized autocorrelation functions indicates that the relaxation is nonexponential and the clusters are not freely moving via Brownian motion but are likely exhibiting some degree of interconnectivity.

In order to investigate structural arrangements of these interconnected clusters, we performed SAXS as well as static light scattering on subtilisin solutions at 55 °C. The measured scattering intensities are shown in Figure 3. The presence of large-scale structures over length scales of at least 2 orders of magnitude larger than the dimension of the monomeric subtilisin can be clearly seen from combined SAXS and static light scattering data.

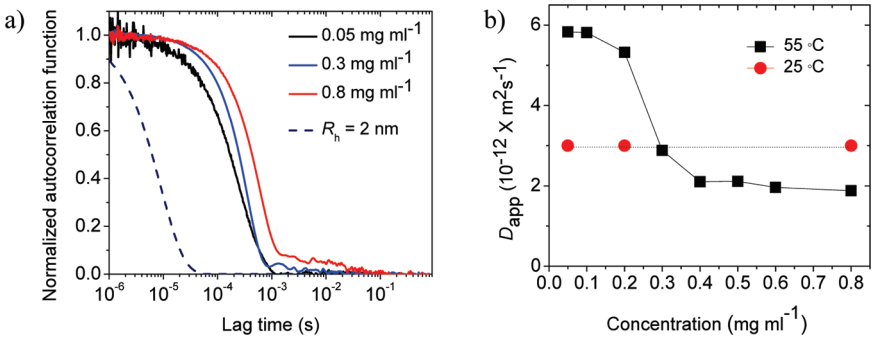

Figure 2. (a) Normalized autocorrelation functions (dimensionless) from dynamic light scattering measurements for various subtilisin concentrations in phosphate buffer at 55 °C along with the calculated autocorrelation function for monomeric subtilisin (R_h = 2 nm). (b) Apparent diffusion coefficients measured for various subtilisin concentrations at 25 and 55 °C.

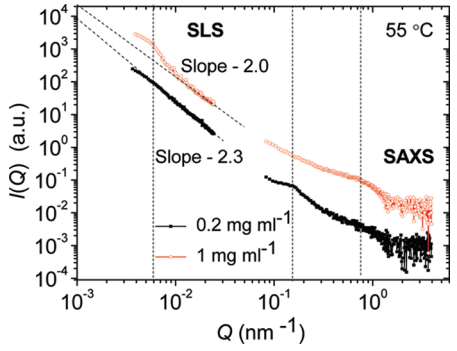

Figure 3. SAXS and static light scattering intensities (in au) for 0.2 and 1 mg mL^{-1} of subtilisin in phosphate buffer at 55 °C. Characteristic length scales are indicated by vertical dotted lines.

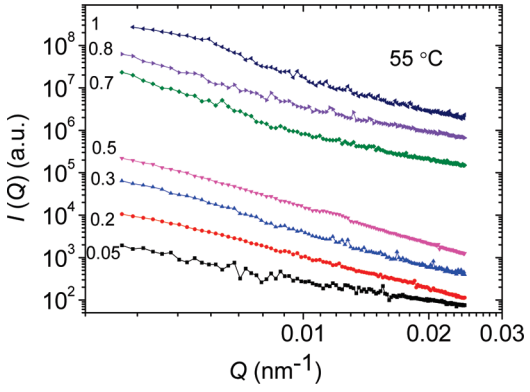

Figure 4. Static light scattering intensities (in au) of different concentrations of subtilisin (in mg mL^{-1} as indicated) in phosphate buffer at 55 °C.

It can also be seen that some characteristic length scales are emerging at various enzyme concentrations, as indicated by vertical dotted lines in Figure 3, at $Q \approx 0.7$ nm^{-1} (corresponding to monomeric subtilisin, cf. Figure 1) for both enzyme concentrations, then at $Q \approx 0.15$ nm^{-1} (length scale about 5 times larger than that of the monomer) at the lower enzyme concentration, and finally at $Q \approx 0.006$ nm^{-1} (length scale about 100 times larger than that of the monomer) at the higher enzyme concentration. The observed length scales indicate a concentration-dependent hierarchical arrangement, where the two smaller length scales correspond to small primary clusters and the longest length scale corresponds to large superclusters. At the lower concentration, the primary cluster length scale corresponds to about 5 times the monomer size, and these primary clusters then appear to be arranged in fractal-like superclusters over at least further two orders magnitude in size. At the higher concentration, primary clusters appear to be smaller, close to the subtilisin monomer length scale, and these are then arranged in fractal-like superclusters with a characteristic length scale about 100 times larger than that of the monomer.

In order to further characterize the structure of these large-scale networks of enzyme clusters, we have used static light scattering measurements over a wide range of enzyme concentrations at 55 °C. The background-corrected static light scattering intensities for various concentrations are shown in Figure 4.

The scattering curves show varying power law behavior with increasing enzyme concentrations, indicating that the enzyme clusters have long-range structures with varying degrees of compactness. At the lowest subtilisin concentration (0.05 mg mL^{-1}), the power law exponent was found to be 1.8, which indicates that the enzyme clusters form fairly open mass fractal structures. The fractal dimension of these supramolecular structures increases to 2.3, 2.6, and 2.6 with increasing enzyme concentration to 0.2, 0.3, and 0.5 mg mL^{-1}, respectively. This indicates that fractal structures become more compact and presumably more rigid with increasing subtilisin concentration.

A structural transition for these fractal structures can be observed at concentrations higher than 0.5 mg mL^{-1}. The shape of the scattering curves is markedly different at higher concentrations (0.7, 0.8, and 1 mg mL^{-1}), where it shows a more complex, multiscale structure with a lower value of the power law scaling exponent (around 2.0) at intermediate Q values (0.01−0.1 nm^{-1}; see Figure 3), as well as an emergence of a characteristic length scale at Q around 0.006 nm^{-1}, which is not seen at lower enzyme concentrations (cf. Figure 3). This is consistent with a structural rearrangement of cluster networking, which is also reflected in the decreased initial decay rate Γ, reflecting the internal dynamics of relaxation of supramolecular structures rather than diffusivity due to Brownian motion of freely diffusing clusters.[18] While we are not aiming here to develop a more detailed structural model of these observed multiscale hierarchical arrangements of enzyme clusters, it is clear that their structure can be systematically controlled by enzyme concentration and temperature.

We have, for the first time, shown direct evidence of long-range supramolecular structures in biocatalyst solutions and demonstrated structural transition in the supramolecular arrangement on submicrometer length scales. The supramolecular structures of enzymes play an important role in biocatalytic-induced

dx.doi.org/10.1021/jz200446j |J. Phys. Chem. Lett. 2011, 2, 1395–1399

self-assembly of short peptide derivatives. We have recently shown that libraries of structurally diverse molecular and network assemblies of Fmoc−dipeptide methyl ester can be achieved simply by varying the concentration of the enzyme. The underlying mechanism for this rich and complex behavior of the self-assemblies is based on the supramolecular structures of the enzyme clusters themselves, which act as catalytic and geometric templates and control the morphology of the supramolecular self-assembly of aromatic peptide amphiphiles by providing a structural environment for catalysis. It is tempting to hypothesize that biocatalytic supramolecular self-assemblies can be controlled not only by tuning the molecular structure of building blocks but also by modulating the interactions of enzyme molecules themselves.

EXPERIMENTAL SECTION

Subtilisin solutions were prepared by mixing and vortexing of 1.25, 5, 8, 12.5, 15, 17.5, 20, and 25 μL of subtilisin stock solution (Sigma Aldrich, Catalogue number P4860; Lot 056K1213) per mL of 100 mM phosphate buffer (pH = 8, filtered with a 0.25 μm Anotop filter), which yielded enzyme solutions at concentrations of 0.05, 0.2, 0.3, 0.5, 0.6, 0.7, 0.8, and 1 mg mL^{-1}. These concentrations correspond to 1.5, 6, 9.6, 15, 18, 24, and 30 U mL^{-1}, expressed in activity units used in our previous report.[3]

SAXS measurements were carried out at Beamline 7T-MPW-SAXS[19] at BESSY II synchrotron source in Berlin, Germany, using an X-ray energy of 9650 eV. Enzyme solutions at various concentrations as well as pure buffer (as background) were injected in glass capillaries and placed in a capillary holder. The capillary holder was then mounted on the sample cell chamber, evacuated, and heated to 25 or 55 °C. The individual samples were then exposed to the X-ray beam to record scattering intensity patterns by using a gas detector placed in the vacuum chamber. The integration and processing of the scattering data was carried out by using the software provided at the beamline.

Static and dynamic light scattering measurements were carried out using the 3DDLS instrument (LS instruments, Fribourg, Switzerland) using vertically polarized He−Ne laser light (25 mW with a wavelength of 632.8 nm) with an avalanche photodiode detector at angles between 15 and 135° at 55 °C. The background scattering intensities (from pure buffer) were subtracted from the scattering intensities of the enzyme solutions. At each scattering angle, dynamic light scattering measurements were also performed by recording the intensity autocorrelation function $g_2(\tau)$ as a function of lag time τ. The autocorrelation functions were analyzed by means of the cumulant method in order to determine the initial decay rate and the corresponding average apparent diffusion coefficient D_{app}.[18] The decay of the normalized autocorrelation function was modeled as $g_1(\tau) = (g_2(\tau) - 1)^{1/2} = \exp(-\Gamma\tau)$, where $\Gamma = D_{app}Q^2$ is the initial decay rate, $Q = (4\pi n/\lambda)\sin(\theta/2)$ is the scattering vector magnitude, n is the refractive index of the solvent, and λ is the wavelength of the laser. The average hydrodynamic radius R_h can be calculated from the Stokes−Einstein equation, $R_h = k_BT/6\pi\eta D_{app}$, where k_B is the Boltzmann constant, T is the absolute temperature, and η is the solvent viscosity at the given temperature.

The scattering intensity patterns from static light and X-ray scattering experiments can be described as $I(Q) \approx KP(Q)S(Q)$, where K is an instrument- and sample-dependent constant, $P(Q)$ is the form factor, which depends on the size and shape of the primary particles, and $S(Q)$ is the structure factor giving information about the spatial arrangement of the primary particles at length scales larger than that of the primary particles (radius of R_p). Please note that $Q = (4\pi/\lambda)\sin(\theta/2)$ for SAXS measurements. In the limit of $QR_g < 1$, the mean radius of gyration R_g of randomly distributed (e.g., freely diffusing) primary particles or clusters can be determined from the measured scattered intensity $I(Q)$ by using the Guinier analysis.[20] In the limit of $1/R_g \ll Q \ll 1/R_p$, where R_g is the mean radius of gyration of a sufficiently large cluster composed of primary particles with radius R_p, the structure factor for fractal clusters with fractal dimension d_f scales with Q through a power law relation as $I(Q) \approx S(Q) \approx Q^{-d_f}$.

ACKNOWLEDGMENT

R.V.U. would like to acknowledge the EPSRC (Advanced Research Fellowship) and Leverhulme Trust (Leadership Award). N.J. would like to acknowledge the Leverhulme Trust and the European Research Council. A.H.R. would like to acknowledge the Leverhulme Trust. We would like to acknowledge the Helmholtz-Zentrum Berlin/Electron storage ring BESSY II for provision of synchrotron radiation at beamline 7T-MPW-SAXS and would like to thank Sylvio Haas for assistance.

AUTHOR INFORMATION

Corresponding Author

*E-mail: jan.sefcik@strath.ac.uk.

REFERENCES

(1) Yang, Z.; Liang, G.; Xu, B. Enzymatic Control of the Self-Assembly of Small Molecules: A New Way to Generate Supramolecular Hydrogels. *Soft Matter* **2007**, *3*, 515–520.

(2) Williams, R. J.; Mart, R. J.; Ulijn, R. V. Exploiting Biocatalysis in Peptide Self-Assembly. *Biopolymers* **2009**, *94*, 107–117.

(3) Hirst, A.; Roy, S.; Arora, M.; Das, A. K.; Hodson, N.; Murray, P.; Marshall, S.; Javid, N.; Sefcik, J.; Boekhoven, J.; et al. Biocatalytic Induction of Supramolecular Order. *Nat. Chem.* **2010**, *2*, 1089–1094.

(4) Mahler, A.; Reches, M.; Rechter, M.; Cohen, S.; Gazit, E. Rigid, Self-Assembled Hydrogel Composed of a Modified Aromatic Dipeptide. *Adv. Mater.* **2006**, *18*, 1365–1370.

(5) Jayawarna, V.; Ali, M.; Jowitt, T. A.; Miller, A. F.; Saiani, A.; Gough, J. E.; Ulijn, R. V. Nanostructured Hydrogels for Three-Dimensional Cell Culture Through Self-Assembly of Fluorenylmethoxycarbonyl-Dipeptides. *Adv. Mater.* **2006**, *18*, 611–614.

(6) Zhang, Y.; Gu, H. W.; Yang, Z. M.; Xu, B. Supramolecular Hydrogels Respond to Ligand−Receptor Interaction. *J. Am. Chem. Soc.* **2003**, *125*, 13680–13681.

(7) Whitesides, G. M.; Boncheva, M. Beyond Molecules: Self-Assembly of Mesoscopic and Macroscopic Components. *Proc. Natl. Acad. Sci. U.S.A.* **2002**, *99*, 4769–4774.

(8) Haines-Butterick, L.; Rajagopal, K.; Branco, M.; Salick, D.; Rughani, R.; Pilarz, M.; Lamm, M. S.; Pochan, D. J.; Schneider, J. P. Controlling Hydrogelation Kinetics by Peptide Design for Three-Dimensional Encapsulation and Injectable Delivery of Cells. *Proc. Natl. Acad. Sci. U.S.A.* **2007**, *104*, 7791–7796.

(9) Williams, R. J.; Smith, A. M.; Collins, R.; Hodson, N.; Das, A. K.; Ulijn, R. V. Enzyme-Assisted Self-Assembly under Thermodynamic Control. *Nat. Nanotechnol.* **2009**, *4*, 19–24.

(10) de la Rica, R.; Matsui, H. Urease as a Nanoreactor for Growing Crystalline ZnO Nanoshells at Room Temperature. *Angew. Chem., Int. Ed.* **2008**, *47*, 5415–5417.

(11) Javid, N.; Vogtt, K.; Krywka, C.; Tolan, M.; Winter, R. Capturing the Interaction Potential of Amyloidogenic Proteins. *Phys. Rev. Lett.* **2007**, *99*, 028101.

(12) Stradner, A.; Sedgwick, H.; Cardinaux, F.; Poon, W. C. K.; Egelhaaf, S. U.; Schurtenberger, P. Equilibrium Cluster Formation in Concentrated Protein Solutions and Colloids. *Nature* **2004**, *432*, 492–495.

(13) Pan, W. C.; Filobelo, L.; Pham, N. D. Q.; Galkin, O.; Uzunova, V. V.; Vekilov, P. G. Viscoelasticity in Homogeneous Protein Solutions. *Phys. Rev. Lett.* **2009**, *102*, 058101.

(14) Hudmon, A.; Kim, S. A.; Kolb, S. J.; Stoops, J. K.; Waxham, M. N. Light Scattering and Transmission Electron Microscopy Studies Reveal a Mechanism for Calcium/Calmodulin-Dependent Protein Kinase II Self-Association. *J. Neurochem.* **2001**, *76*, 1364–1375.

(15) Akbar, U.; Aschenbrenner, C. D.; Harper, M. R.; Johnson, H. R.; Dordick, J. S.; Clark, D. S. Direct Solubilization of Enzyme Aggregates with Enhanced Activity in Nonaqueous Media. *Biotechnol. Bioeng.* **2007**, *96*, 1030–1039.

(16) Ehrlich, H.; Deutzmann, R.; Brunner, E.; Cappelini, E.; Koon, H.; Solazzo, C.; Yang, Y.; Ashford, D.; Thomas-Oates, J.; Lubeck, M.; et al. Mineralization of the Metre-Long Biosilica Structures of Glass Sponge is Templated on Hydroxylated Collagen. *Nat. Chem.* **2010**, *2*, 1084–1088.

(17) Svergun, D.; Barberato, C.; Koch, M. H. J. CRYSOL — A Program to Evaluate X-ray Solution Scattering of Biological Macromolecules from Atomic Coordinates. *J. Appl. Crystallogr.* **1995**, *28*, 768–773.

(18) Sandkuhler, P.; Lattuada, M.; Wu, H.; Sefcik, J.; Morbidelli, M. Further Insights into the Universality of Colloidal Aggregation. *Adv. Colloid Interface Sci.* **2005**, *113*, 65–83.

(19) Hoell, A.; Zizak, I.; Bieder, H.; Mokrani, L. German Patent DE 10 2006 029 449, 2006.

(20) Guilbaud, J. B.; Saiani, A. Using Small Angle Scattering (SAS) to Structurally Characterise Peptide and Protein Self-Assembled Materials. *Chem. Soc. Rev.* **2011**, *40*, 1200–1210.